

# Synthesis, Characterization, and Growth Mechanism of Self-Assembled Dendritic CdS Nanorods

Lifeng Dong, Tatyana Gushtyuk, and Jun Jiao\*

Department of Physics, Portland State University, Portland, Oregon 97207-0751

Received: August 20, 2003

A simple evaporation-condensation method was used to investigate self-assembled CdS nanorods with different geometrical configurations. At the evaporation temperature of 800 °C, the growth of branched CdS structures with multi nanorod arms along the [0001] direction was observed. However, at 1000 °C, dendritic arrays of parallel CdS nanorods were formed along the [0001] direction. The diameters of the nanorods range from 30 to 500 nm and their lengths from 1 to 5  $\mu\text{m}$ . A series of electron microscopy characterization results suggests that the growth of both types of CdS nanorods is governed by the vapor-solid growth mechanism. The formation of CdS nanorods with various morphologies is attributed to the intrinsically anisotropic growth of wurtzite CdS structure along the [0001] *c* axis as well as the varying supersaturation of CdS vapor with the evaporation temperature.

## Introduction

Due to its nonlinear properties, CdS, one of the most important II–VI group semiconductors, has been investigated as the building blocks for nanoscale laser light-emitting diodes and optical devices. A number of methods have been explored to grow CdS nanocrystals,<sup>1,2</sup> nanowires/nanorods,<sup>3–7</sup> and nanobelts.<sup>7</sup> Recently, electrically driven laser properties have been demonstrated on a single CdS nanowire.<sup>8</sup> However, for the realization of a functional CdS nanosystem, the challenge is to find a novel method to hierarchically assemble the nanoscale CdS building blocks. In this paper, we report a simple evaporation-condensation method to synthesize self-assembled dendritic CdS nanorods with different geometrical configurations. The growth mechanism of dendritic CdS nanorods is discussed on the basis of the thermodynamics and kinetics of crystal growth. In particular, our study suggests that the architecture of CdS nanorods is directly related to the evaporation temperature. The synthesis of self-assembled CdS nanorods is a crucial step toward the realization of nanoscale CdS laser diodes and other optoelectronic devices. It is expected that the dendritic growth of CdS nanorods into microscale structures will provide opportunities for the study of optical interference, coupling, and other possible nonlinear collective effects of nanoscale CdS devices.<sup>9</sup>

## Experimental Section

**Preparation of Substrates.** Unlike previous reports in which silicon (Si) wafers were usually used as the substrate for the growth of carbon nanotubes and semiconductor nanowires, in our experiments, we utilized tungsten (W) foil as the growth substrate. This is because W is a refractory support material for electron field emitters due to its high melting point and stability in various environments.<sup>10</sup> Also, there is no interaction between the W substrate and CdS. We have reported that when using Si wafer as the substrate to grow CdS nanostructures,

SiO<sub>x</sub>/CdS composite nanowires and nanobelts were synthesized due to the interactions between CdS and the Si substrate.<sup>11</sup> Prior to use as the growth substrate, the W foils (Alfa Aesar, 99.95%) were polished, ultrasonicated in acetone for 5 min, rinsed with deionized water, and then dried with flowing nitrogen (N<sub>2</sub>) gas.

**Growth of Self-Assembled Dendritic CdS Nanorods.** The synthesis of self-assembled CdS nanorods was based on the evaporation-condensation of CdS powder. The growth of large CdS crystals usually occurs between 800 and 1000 °C, safely below the softening point of a quartz tube.<sup>12</sup> Therefore, in our experiment, CdS powder was evaporated at both 800 and 1000 °C. Before the evaporation–condensation process, the CdS powder (Aldrich; purity, 99.995%; grain size, <5  $\mu\text{m}$ ) was placed on a ceramic plate in the center of a quartz tube, which was located in a horizontal tube furnace. Several pieces of W foils were placed downstream of the gas flow close to the ceramic plate. After this, the quartz tube was sealed and evacuated to a vacuum of  $3 \times 10^{-3}$  Torr. Then, the chamber was filled with flowing argon gas to 150 Torr and the furnace was heated at a rate of 20 °C per minute. When the system reached the desired evaporation temperature of 800 or 1000 °C, the process of synthesizing CdS nanorods was maintained for 60 min at 150 Torr with the flowing argon gas at 150 cm<sup>3</sup>/min. After the growth process, the chamber pressure was set to 375 Torr of argon gas, and the system was allowed to cool to room temperature.

**Electron Microscopy Characterization.** The morphologies of the as-synthesized CdS nanorods were examined using an FEI Sirion field emission scanning electron microscope (FESEM). To facilitate investigation of the detailed surface morphology of CdS nanorods, no conductive metal layer such as Au, Pd/Au, Cr, or carbon layer was coated on the sample surface. To avoid surface charging, the FESEM was operated at the low acceleration voltage of 1–2 kV. At this low acceleration voltage range, the depth of the interaction between the incident electron beam and the surface of CdS nanorods is small, thus allowing us to observe the fine surface structure of the CdS nanorods.

\* To whom correspondence should be addressed. E-mail: jiao@pdx.edu. Tel: +1-503-725-4228. Fax: +1-503-725-9525.

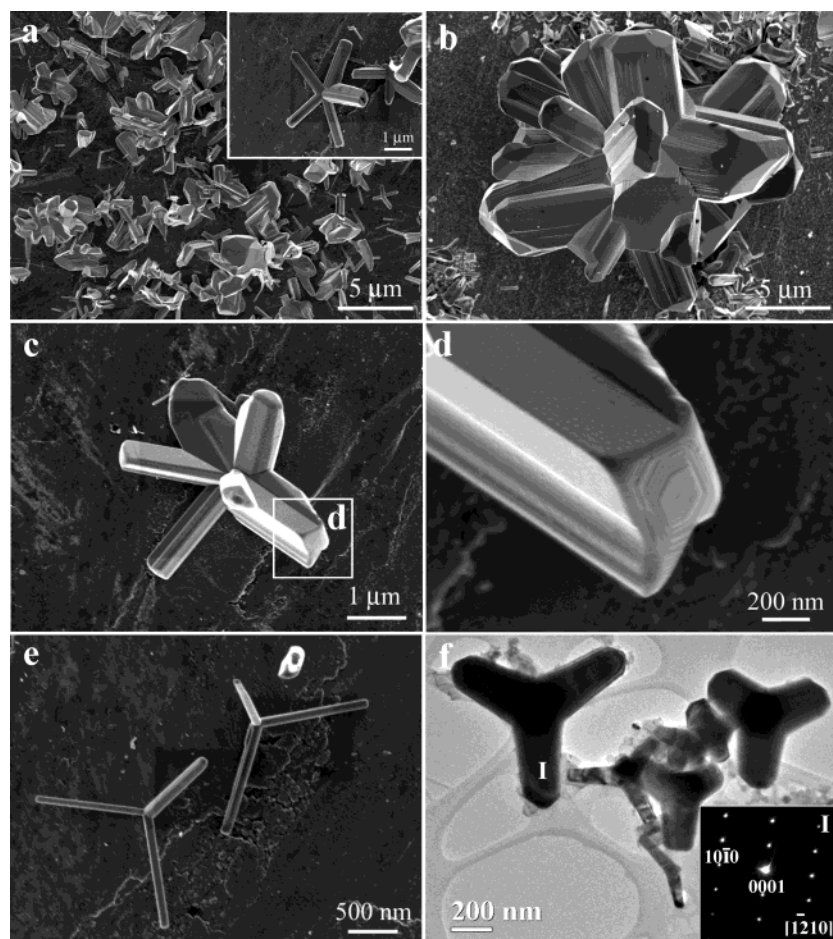


**Figure 1.** a–e. SEM images of branched CdS nanorods with different geometrical configuration. Figure 1f. TEM image of CdS tripods (inset: SAED pattern taken from the region labeled as I in Figure f.)

An FEI Tecnai F-20 field emission high-resolution transmission electron microscope (HRTEM) equipped with an energy-dispersive X-ray (EDX) spectrometer was used to characterize the internal structures of CdS nanorods and to analyze their elemental compositions. To prepare the HRTEM samples, CdS nanorods were carefully scraped from the surface of the W substrates, dispersed in an ethanol solution, and ultrasonicated for 5 min. Several drops of suspension were then transferred onto a holey carbon TEM copper grid.

## Results and Discussion

After the growth process at the evaporation temperature of 800 °C, the W substrates were found to be coated with a thin layer of yellow powder. A representative SEM image of as-synthesized yellow products (Figure 1a) shows that mixtures of branched CdS structures with multi nanorod arms and micro CdS crystals were formed on the W substrate. The diameter of nanorods ranges from 50 to 500 nm. Some micro rods with diameters at several  $\mu\text{m}$  were also observed (Figure 1b). As shown in Figure 1, parts b and e, as their size increases, the shape of dendritic CdS branches changes from a cylindrical to a faceted rod shape. Furthermore, some CdS structures with symmetrically distributed nanorod branches were observed, such as branched bipod- (Figure 1a), tripod- (Figure 1e), tetrapod- (Figure 1a), heptapod- (inset of Figure 1a), and hexapod-shaped (Figure 1c) nanorods. The SEM image of one end of a CdS hexapod (Figure 1d) clearly demonstrates that there is a hexagonal step (screw dislocation) located at the tip. This growth

phenomenon indicates that it is the screw dislocation at the nanorod tip that leads the growth of the CdS nanorod, and the nanorod growth is controlled by the vapor-solid (VS) growth mechanism.<sup>13,14</sup> This means that the CdS vapor, evaporated from the CdS powder precursor at the temperature of 800 °C, directly deposits on the W substrate in the downstream region and self-assembles into branched nanorods. Such an axial screw dislocation at the growing tip provides a preferred growth site and accounts for unidirectional growth.<sup>14</sup> The selected area electron diffraction (SAED) patterns obtained from the CdS nanorods show that all of the CdS nanorods grow along the [0001] direction instead of the symmetric distribution of CdS nanorods along different geometrical directions. This is evident in a SAED pattern taken from the downward branch of a tri-pod (labeled as I in Figure 1f) as shown in the inset of Figure 1f.

We have found that with the presence of Au catalyst, CdS nanostructures could be synthesized along the direction  $[10\bar{1}0]$  instead of [0001]. When the W substrates were coated with a Au film of  $\sim 20$  nm thickness and the other growth conditions were kept the same, both CdS nanowires and CdS nanobelts were formed along the direction  $[10\bar{1}0]$ .<sup>7</sup> Duan and Lieber also observed that using a laser-assisted catalytic growth method and Au as the catalyst, CdS nanowires formed along both directions of  $[10\bar{1}0]$  and [0001].<sup>3</sup> However, without the aid of Au catalyst, on the basis of the thermodynamics and kinetics of crystal growth, the favored growth direction for the wurtzite CdS nanorods is along the [0001] axis and not along the  $[10\bar{1}0]$  axis. This is because, for the hexagonal wurtzite crystal structure,  $\{10\bar{1}0\}$  planes are energetically more stable than  $\{0001\}$  planes,

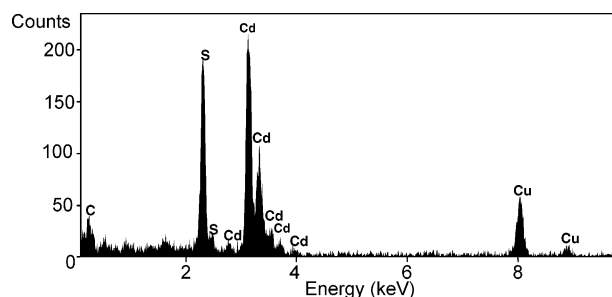


**Figure 2.** EDX spectrum obtained from the nanorod region, which confirms the compositions of CdS nanorods.

and the growth rate of  $\{0001\}$  planes is faster in comparison to that of  $\{10\bar{1}0\}$  planes.

The composition of the nanorods and micro crystals was examined further using an EDX spectrometer attached to a transmission electron microscope operated at 200 kV. The EDX spectrums obtained from the nanorods and micro crystals are the same. A typical EDX spectrum is presented in Figure 2. The spectrum confirms two things: (a) that both the nanorods and crystals are composed only of Cd and S, and (b) that the W from the substrate was not involved in the formation of CdS nanorods. Both the Cu and C signals in Figure 2 come from the holey carbon TEM copper grid.

To investigate the thermodynamics and kinetics of the growth of dendritic CdS nanorods, in some experiments, CdS powder was evaporated at 1000 °C instead of 800 °C. The comparative experiment indicates that the morphology of self-assembled dendritic CdS structures is related to the evaporation temperature. As shown in Figure 3a–c, at the evaporation temperature of 1000 °C, an array of parallel CdS nanorods was formed on one end or two opposite ends of micro CdS crystals. The growth direction was regardless of the flow direction of the argon gas. This suggests that during the CdS evaporation–condensation process, micro CdS crystals formed first, and then CdS nanorods grew from the preferred facet of the CdS crystals. The diameters of the nanorods range from 50 to 300 nm and their lengths from 1 to 5  $\mu\text{m}$ . Note that the diameter of the nanorods decreases along the growth direction. The size of micro CdS crystals ranges from 1 to 80  $\mu\text{m}$ . Also, some CdS nanorods with much

smaller diameters were observed to grow on the surface of the micro CdS crystals (Figure 3, parts c and d). It is worth noting that these small nanorods have a uniform diameter of 30 nm along the growth direction. There is a pyramid shaped step between the small nanorod and the CdS crystal as shown in the inset of the Figure 3d. As demonstrated in Figure 3c, both types of CdS nanorods were formed parallel to each other. This indicates that the small nanorods (Figure 3, parts c and d) are in an early growth stage of the larger CdS nanorods as shown in Figure 3, parts a and b. With an increase of growth time, the small nanorods grow further and become tapered in the growth direction. As predicted by the VS growth mechanism,<sup>13</sup> while the axial growth of CdS nanorods occurs, the CdS vapor also directly deposits on the surface of previously formed nanorod segment. This is responsible for the radial growth of CdS nanorods. Because the axial growth rate is faster than that of radial growth, the combined processes result in the formation of CdS nanorods with tapered tips.

HRTEM images and SAED patterns obtained from the CdS nanorods and micro crystals clearly demonstrate the monolithic single-crystalline nature of the entire dendritic CdS array structure. Figure 4a is a representative TEM image of the structure. CdS nanorods are self-assembled parallel to each other along the same growth direction. The HRTEM images of Figure 4b–d were taken from different areas of the dendritic CdS structure as labeled in Figure 4a. As shown in Figure 4b, there are no crystallization defects in the interface area between a CdS nanorod and the micro crystal, thus indicating monolithic growth from the micro CdS crystal base. To further confirm this monolithic growth phenomenon, SAED patterns were taken from both the crystal base (labeled as I) and the nanorod (labeled as II). As shown on the right-hand side of Figure 4b, the SAED patterns from both regions are exactly the same. This further confirms the monolithic growth of the CdS nanorods. Also, both HRTEM images and SAED patterns demonstrate the wurtzite structure of the entire CdS dendritic structure. The lattice spacing of  $3.36 \pm 0.05$  Å between adjacent lattice planes in Figure 4b–d corresponds to the distance between two (0002) crystal planes, confirming [0001] as the preferred growth direction for the wurtzite CdS nanorods. This is consistent with previous reports

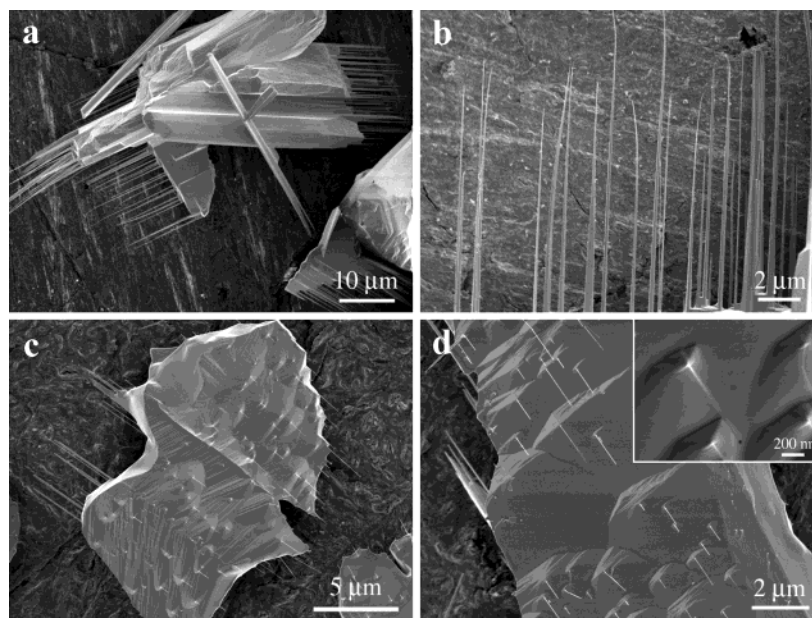


**Figure 3.** a and b. SEM images of self-assembly CdS nanorods formed on the micro CdS crystals. c and d. SEM images of small self-assembly CdS nanorods, which are in the early stage of the formation of nanorods shown in parts a and b.



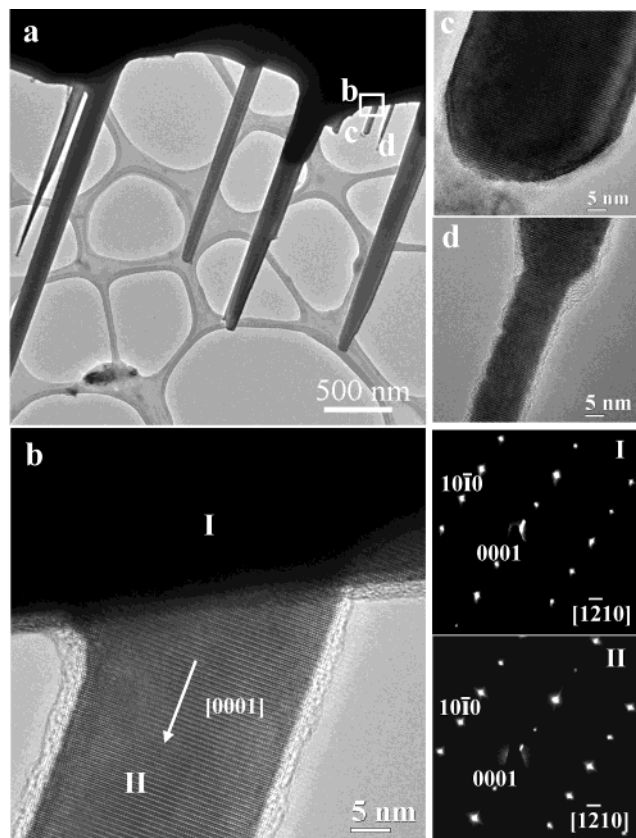


**Figure 4.** a. TEM image of a typical CdS dendritic structure. b–d. HRTEM images taken from different regions of the CdS dendritic structure in part a. Right of part b. SAED patterns taken from the micro CdS crystal I (up) and CdS nanorod region II (bottom).

that, at 800–1000 °C, CdS crystals were formed only as wurtzite phase.<sup>1,12</sup> As shown in Figure 4c, the diameter of the nanorod is about 50 nm, and the nanorod tip has a polyhedral shape. There is a thin amorphous layer on the surface of each nanorod (Figure 4b–d). A relatively thicker amorphous layer exists on the transition region where the rod has two different diameters (Figure 4d).

With regard to the geometrical shape of the dendritic CdS nanorods, our experimental results demonstrate that, at 1000 °C, the CdS nanorods tend to align themselves parallel to each other, whereas at 800 °C, no such self-assembly array occurs, but instead, the CdS nanorods are branched. This is due to the anisotropy of the vapor-solid deposition rate as a function of temperature. As we know, wurtzite CdS is intrinsically an anisotropic material with a unique *c* axis, and when other parameters (pressure, gas flow rate) are kept constant, the supersaturation of CdS vapor increases with the evaporation temperature. When the system is kinetically driven by a high supersaturation of CdS at 1000 °C, the growth of CdS nanorods with the wurtzite structure is highly anisotropic. In this case, the growth rate is generally faster along the *c* axis [0001]; the result is a rodlike faceted nucleus where the long axis is the *c* axis of the wurtzite crystal structure. Subsequently, the nanorods are monolithically formed on one or both ends of the rodlike

faceted nucleus. At 800 °C, the overall growth rate is slow due to the low supersaturation. To minimize surface area, a nearly spherical, but still faceted CdS nucleus forms. Then nanorods grow symmetrically from the facets of the CdS nucleus. Based on the thermodynamics and kinetics of crystal growth, the above simple evaporation-condensation method could be developed to synthesize other II–VI group semiconductors such as CdSe, ZnS, ZnO, ZnSe, and ZnTe due to their anisotropic crystal structure of the hexagonal wurtzite phase.

## Conclusions

On the basis of the evaporation–condensation of CdS powder, a simple and efficient method was investigated to monolithically grow dendritic CdS nanorods from micro CdS crystals. Due to the anisotropic growth rate of wurtzite CdS nanorods along the *c* axis [0001], various morphologies of CdS nanorods were formed at the different evaporation temperatures. With the increase of the evaporation temperature, the anisotropic growth rate is faster along the [0001] direction. Thus, at 1000 °C, rod like CdS nuclei were formed along the [0001] direction, and an array of parallel CdS nanorods grew monolithically from the rod like faceted CdS nucleus. At 800 °C, the formation of a nearly spherical, yet faceted CdS nucleus promotes the growth of branched CdS nanorods, such as CdS bipods, tripods, tetrapods, heptapods, and hexapods. Despite the varying morphology due to the evaporation temperature, all of the nanorods grow along the [0001] direction, and the growth process is governed by the VS growth mechanism. The self-assembly growth of dendritic CdS nanorods is an important step toward the fabrication of CdS nanoscale optoelectronic devices.

**Acknowledgment.** This work was supported in part by the National Science Foundation (DMR-0097575 and ECS-0217061) and American Chemical Society Petroleum Research Fund (PRF-38108-G5).

## References and Notes

- (1) Jun, Y.; Lee, S.; Kang, N.; Cheon, J. *J. Am. Chem. Soc.* **2001**, *123*, 5150.
- (2) Peng, Z. A.; Peng, X. G. *J. Am. Chem. Soc.* **2001**, *123*, 183.
- (3) Duan, X. F.; Lieber, C. M. *Adv. Mater.* **2000**, *12*, 298.
- (4) Xu, D. S.; Xu, Y. J.; Chen, D. P.; Guo, G. L.; Gui, L. L.; Tang, Y. Q. *Adv. Mater.* **2000**, *12*, 520.
- (5) Routkevitch, D.; Bigioni, T.; Moskovits, M.; Xu, J. M. *J. Phys. Chem.* **1996**, *100*, 14037.
- (6) Zhan, J. H.; Yang, X. G.; Wang, D. W.; Li, S. D.; Xie, Y.; Xia, Y. N.; Qian, Y. T. *Adv. Mater.* **2000**, *12*, 1348.
- (7) Dong, L. F.; Jiao, J.; Coulter, M.; Love, L. *Chem Phys. Lett.* **2003**, *376*, 653.
- (8) Duan, X. F.; Huang, Y.; Agarwal, R.; Lieber, C. M. *Nature* **2003**, *421*, 241.
- (9) Yan, H. Q.; He, R. R.; Johnson, J.; Law, M.; Saykally, R. J.; Yang, P. D. *J. Am. Chem. Soc.* **2003**, *125*, 4728.
- (10) Dong, L. F.; Jiao, J.; Tuggle, D. W.; Petty, J.; Elliff, S. A.; Coulter, M. *Appl. Phys. Lett.* **2003**, *82*, 1096.
- (11) Jiao, J.; Dong, L. F.; Tuggle, D. W.; Petty, J.; Love, L.; Coulter, M. *Mater. Res. Soc. Symp. Proc.* **2003**, *739*(H5.4).
- (12) Gilman, J. J. *The Art and Science of Growing Crystals*; John Wiley & Sons: New York, 1963.
- (13) Sears, G. W. *Acta Metal.* **1955**, *3*, 361.
- (14) Levitt, A. P. *Whisker Technology*; John Wiley & Sons: New York, 1970.